sediments and K is a constant factor. Following (29), we let $K = 10^3$, and assume $a = 10^{-7}$ m, which is comparable to the size of typical clay particles.
37. J. X. Mitrovica, A. M. Forte, *J. Geophys. Res.* **102**, 2751 (1997).
38. G. A. de Wijs *et al.*, *Nature* **392**, 805 (1998).
39. A. D. Brandon *et al.*, *Science* **280**, 1570 (1998).
40. Archie's law defines the electrical conductivity of the porous sediments as $\sigma = \phi^n \sigma_c$, where $\sigma_c = 5 \times 10^5$ S m^{-1} is the electrical conductivity of liquid iron and n is a constant that typically lies between 1 and 2. We choose $n = 1.5$ in our calculations.
41. The P- and S-wave velocities are based on the Hashin-Shtrikman bounds for elastic composites. We plot the upper bounds so that our velocity reductions represent minimum values. [J. P. Watt, G. F. Davies, R. J. O'Connell, *Rev. Geophys.* **14**, 541 (1976)]. The sediment properties are based on the mantle properties in (26). The P-wave velocity in the liquid is $v_c^P = 8.06$ km s^{-1}.
42. P. M. Mathews, B. A. Buffett, T. A. Herring, in preparation.
43. E. J. Garnero, J. E. Vidale, *Geophys. Res. Lett.* **26**, 377 (1999).
44. J. C. Castle, R. D. van der Hilst, *Earth Planet. Sci. Lett.* **176**, 311 (2000).
45. The rejection of light elements from the inner core provides an important source of buoyancy for convection in the core. Light elements at the inner-core boundary $r = r_{ic}$ are mixed into the volume of the outer core. The release of gravitational energy is proportional to $\bar{\psi} - \psi(r_{ic})$, where $\psi(r_{ic})$ is the gravitational potential at $r = r_{ic}$ and $\bar{\psi}$ is the average potential over the liquid core. If the excess light elements are subsequently incorporated into sediments at the top of the core $r = r_c$, the total release of gravitational energy is proportional to $\psi(r_c) - \psi(r_{ic})$, which is larger than $\bar{\psi} - \psi(r_{ic})$ by about a factor of 2.
46. Partially supported by NSERC (B.A.B.), NSF, the UC Institute of Geophysics (R.J.), and NSF grants EAR-9905710 and NSF-9996302 (E.J.G.).

22 June 2000; accepted 29 September 2000

Regional Changes in Carbon Dioxide Fluxes of Land and Oceans Since 1980

Philippe Bousquet,[1,2]* Philippe Peylin,[1] Philippe Ciais,[1] Corinne Le Quéré,[1]† Pierre Friedlingstein,[1] Pieter P. Tans[3]

We have applied an inverse model to 20 years of atmospheric carbon dioxide measurements to infer yearly changes in the regional carbon balance of oceans and continents. The model indicates that global terrestrial carbon fluxes were approximately twice as variable as ocean fluxes between 1980 and 1998. Tropical land ecosystems contributed most of the interannual changes in Earth's carbon balance over the 1980s, whereas northern mid- and high-latitude land ecosystems dominated from 1990 to 1995. Strongly enhanced uptake of carbon was found over North America during the 1992–1993 period compared to 1989–1990.

Over the past two decades, on average, about half of the CO_2 emissions caused by fossil fuel combustion have remained in the atmosphere, the rest having been absorbed by the ocean and by land ecosystems. Year-to-year variations in the rate of atmospheric CO_2 accumulation are of the same magnitude as the decadal mean annual accumulation and result primarily from shifts in the natural carbon fluxes (*1*). Previous investigations into which reservoir (land or ocean) and which regions caused such year-to-year changes have produced conflicting answers. Carbon stable isotope studies all infer large shifts of both land and ocean fluxes of up to several gigatonnes (10^{15} g) of carbon per year (GtC year^{-1}) (*2, 3*). In contrast, ocean carbon models and measurements of the CO_2 partial pressure difference between the ocean surface and the atmosphere (ΔpCO_2) suggest relatively small changes in the air-sea fluxes (*4–6*). Global biogeochemical models of the land biosphere generally produce large interannual shifts in terrestrial fluxes, but they differ in where or how they attribute these shifts to underlying processes (photosynthesis or respiration).

Inverse models using atmospheric CO_2 observations and atmospheric transport have been applied to infer the mean spatial distribution of CO_2 fluxes (*7–9*), but rarely to estimate their interannual variability (*10*). Here, we constructed an inversion using 20 years of atmospheric CO_2 measurements, mostly from the NOAA Climate Monitoring and Diagnostics Laboratory air sampling network, to infer monthly changes in the carbon balance of large regions. The carbon balance of continents and oceans can be considered as the sum of two components, a long-term mean net flux (over 20 years) and a monthly varying flux anomaly. In the following, we present and discuss the monthly varying flux anomalies. The results of the inverse approach ("top-down") are compared with predictions of two state-of-the-art global models ("bottom-up") of the carbon fluxes over land ecosystems and oceans.

Over the past 20 years, the annual accumulation of CO_2 in the atmosphere has varied between 1 and 6 GtC year^{-1} (*1*). Because fossil CO_2 emission changes do not vary much from year to year, the observed changes in accumulation rate reflect variations of ocean and land fluxes. At present, about 120 CO_2 data records from around the globe are available (*11*). Most CO_2 stations are in the marine boundary layer; they can be influenced directly by ocean fluxes and more indirectly by land fluxes. A few CO_2 stations, however, are close to or within the continents and can better capture year-to-year changes in terrestrial fluxes. Among the 120 sites available in 1998, we have selected 67 sites (*12*). At each site, we have analyzed the variance of the deseasonalized trend after subtraction of the trend at the South Pole (*13*). This analysis indicates that there is "excess" variance at low frequency at continental sites compared to oceanic sites (Fig. 1). This excess variance may reflect short-term spatial and temporal variability of land fluxes or of atmospheric transport. However, it also suggests that terrestrial carbon fluxes exhibit larger year-to-year variations than their oceanic counterparts. This inference can be evaluated by using an inverse model to calculate regional carbon balance variations from observed concentration variations.

We have developed such a model, extending the work of (*9*), to retrieve the net CO_2 fluxes every month from 1980 to 1998 (*13*). The inverse model optimizes CO_2 ocean and land fluxes for 11 continental regions and eight ocean regions (Fig. 1) by minimizing the differences between the CO_2 concentrations simulated by a three-dimensional atmospheric transport model and those observed at measurement sites. Fossil CO_2 fluxes are prescribed from energy use statistics (*14*). The control inversion is described in (*13*). The atmospheric CO_2 data used for the inversion are calculated from 67 selected monitoring sites (*12*) over the period 1980–1998. Raw flasks and in situ records are smoothed in the time domain to remove synoptic variability (*11*) and are used in the form of monthly means. An increasing number of stations is available over time, from 20 sites in 1980 to 67 sites in 1997, with 35 new sites appearing between 1987 and 1991. Data uncertainties are estimated each month at each station from the (synoptic) scatter and measurement uncertainties of the original flask data (*13*). In addition to the control inversion (*13*), we have carried out a sensitivity study consisting of seven additional inversions in which key parameters are varied individually (*15*), provid-

[1]Laboratoire des Sciences du Climat et de l'Environnement (LSCE), F-91198 Gif-sur-Yvette Cedex, France. [2]Université de Versailles Saint Quentin en Yvelines (UVSQ), F-78035 Versailles Cedex, France. [3]National Oceanic and Atmospheric Administration (NOAA), Climate Monitoring and Diagnostics Laboratory, Boulder, CO 80303, USA.

*To whom correspondence should be addressed. E-mail: pbousquet@cea.fr

†Present address: Max-Planck-Institut für Biogeochemie, D-07701 Jena, Germany.

ing a range of uncertainty on the inferred fluxes. The sensitivity study was performed to better account for uncertainties that are not explicitly represented in the inverse procedure, which only returns a residual uncertainty.

At the regional scale, we find that the long-term mean net fluxes are significantly different among the eight inversions, within a typical range of 0.4 GtC year^{-1} for ocean regions and of 0.8 GtC year^{-1} for land regions. Independent inverse modeling studies of the mean net fluxes tend to confirm this result (*7–9*). On the other hand, the inferred flux anomalies are substantially more similar among our sensitivity tests, which suggests that anomalies are retrieved more robustly than long-term mean fluxes (*16*). The latter are inferred from mean spatial concentration differences among stations, which are rather small within a given latitude band. For instance, the apportionment of sources and sinks between North America and Eurasia relies on spatial mean differences on the order of 0.5 parts per million (ppm) at mid-northern latitudes (*7*). In contrast, flux anomalies for these regions are inferred from temporal changes of concentration differences between stations, which are larger than mean longitudinal differences (see below). Accordingly, we focus on monthly flux anomalies.

During the 1980–1998 period, land fluxes are found to be twice as variable as ocean fluxes (Fig. 2), in agreement with the qualitative analysis in Fig. 1. The anomalies have a peak-to-peak amplitude of 5.0 GtC for the total global terrestrial flux and 2.5 GtC for the global air-sea flux. Anomalous uptake over land is inferred during 1981–1983, 1991–1993, and 1997, and anomalous uptake over oceans persists from 1989 to 1996. Unlike previous studies that relied on atmospheric carbon isotope records (*2, 3*), we infer no significant anticorrelation in the flux anomalies between ocean and land. In this study, the ocean flux anomalies are always smaller than the land anomalies. The inversion with the minimum variability in the air-sea flux anomalies (half as large as the control run) corresponds to larger observational uncertainties, allowing a looser fit to the ocean stations. The inversion with the maximum variability in the air-sea flux anomalies (1.3 times as large as the control run) occurs when no constraint is applied to the global mean ocean uptake (*13*).

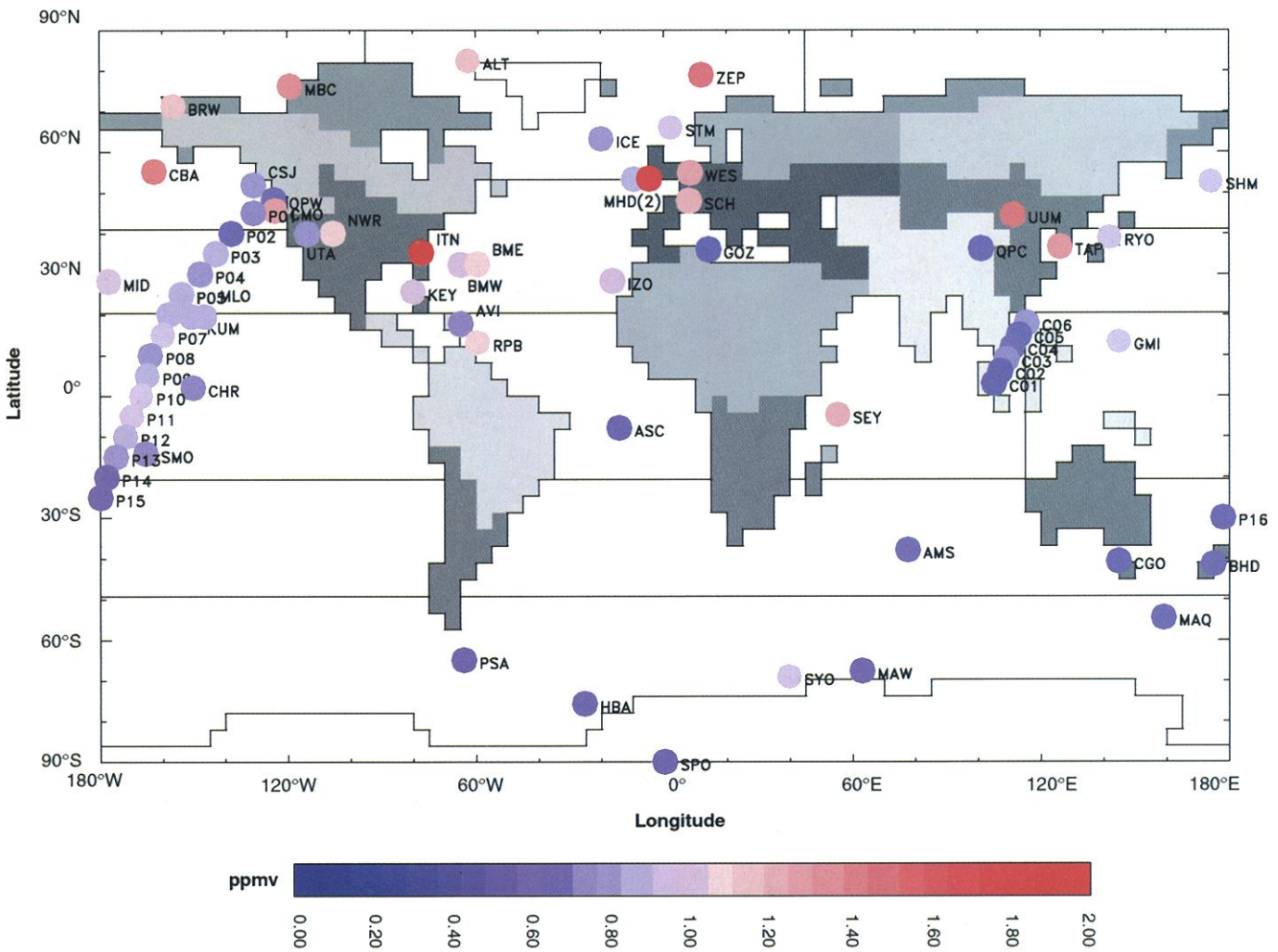

Fig. 1. Year-to-year variability of the CO_2 trend at the monitoring sites used in the inverse procedure over the period 1980–1998. The variability is estimated by the standard deviation of the weekly CO_2 deseasonalized trend after subtraction of the South Pole trend (*13*). Sites further toward the red end of the scale indicate stronger trend variations, which are presumably caused by larger variability of the sources influencing the station. The 11 continental regions (gray areas) and the eight ocean regions (separated by lines) used in the inverse procedure are also shown. For the continents, from north to south: Arctic regions (far North America and far north Eurasia), boreal and temperate North America, boreal and temperate Europe, boreal and temperate North Asia, tropical Africa, south America, tropical Asia, and all lands south of 20°S. For the oceans: North Atlantic, >50°N; North Pacific, >50°N; North Atlantic, 20° to 50°N; North Pacific, 20° to 50°N; Equatorial Pacific, 20°S to 20°N; sum of Equatorial Indian and Atlantic, 20°S to 20°N; subtropical, sub-Antarctic oceans, 20° to 50°S; and Southern Ocean, >50°S. A total of 67 sites are used in this study. The Mace-Head (MHD, Ireland) continuous record is split in two time series according to continental and oceanic origin of air at the station (two dots).

No individual ocean basin is inferred to contribute predominantly to the global ocean flux anomaly, although both the Southern Ocean (south of 50°S) and the equatorial zone exhibit relatively larger flux anomalies. The Equatorial Pacific (20°S to 20°N) is known to exhibit year-to-year variations in the air-sea CO_2 fluxes, as shown by repeated surveys (*17–20*) of measured ΔpCO_2. The year-to-year variations found in our inversions are in good agreement with the ocean flux anomalies derived from ΔpCO_2 measurements (*17–20*). Both approaches estimate an anomalous CO_2 sink of 0.1 to 0.5 GtC year^{-1} during the strong El Niño events of 1982–1983, 1986–1987, and 1997–1998, and an anomalous source of the same amplitude during the La Niña event of 1988–1989. The agreement in this region may be partially due to the relatively dense observational network in the atmosphere, with 20% of the flask data (Fig. 1), and in the ocean with the dense ΔpCO_2 coverage (*17–20*).

Our inversions also compare favorably with the ocean carbon model of (*21*) for the amplitude of the year-to-year variations both in the Equatorial Pacific (Fig. 3A) and in the Southern Ocean [not shown, see (*22*)]. However, some phasing differences remain between the two approaches. Outside the Equatorial Pacific and Southern Ocean, the inversions and the ocean carbon model disagree: The inversions give much larger variations than the ocean model (±0.4 versus ±0.1 GtC year^{-1}). The few basin scale observations do not justify a preference of one estimate over the other. The ocean model could underestimate variability because it does not include continental margins, and because it underestimates the variability in ocean dynamics at high latitudes (*21*). On the other hand, the inversions could overestimate variability because the low density of the atmospheric stations makes it difficult to draw a precise line between land and ocean, leaving the possibility that some of the land variability has been attributed to the oceans.

During the 1980s, tropical land regions are found to contribute more anomalous changes to the global carbon balance than mid- and high-latitude ecosystems, whereas the converse is true for the period 1990–1995. During the period 1996–1998, tropical and Northern Hemisphere land ecosystems contribute equally to the total flux anomaly (*13*). Observed changes in the CO_2 growth rate partly illustrate that result. For the periods 1980–1985, 1989–1991, and 1995, growth rate anomalies start in the tropics and propagate toward high latitudes within a few months. During the period 1992–1993, a negative growth rate anomaly initiates at mid-northern latitudes and then propagates toward the Equator (*13*).

In the 1980s, tropical land regions predominantly influence the carbon flux anomalies in all eight inversions performed (Fig. 3A), except during 1984–1985. An anomalous source is inferred during El Niño years in 1987–1988 and 1998, whereas an anomalous sink occurs during 1982, 1985–1986, and 1989–1993. A strong El Niño occurred in 1982–1983, for which the inversions produce only a relatively small positive flux anomaly over tropical land regions (Fig. 3B). This may reflect the low station

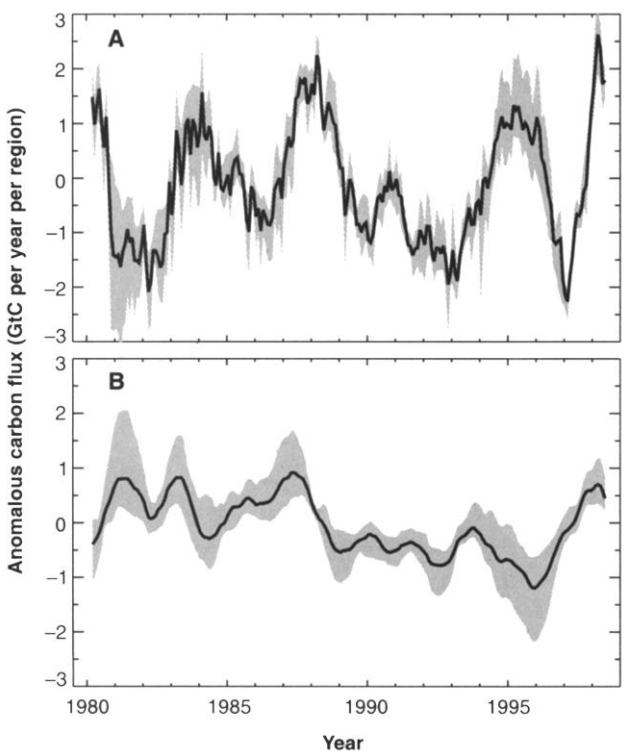

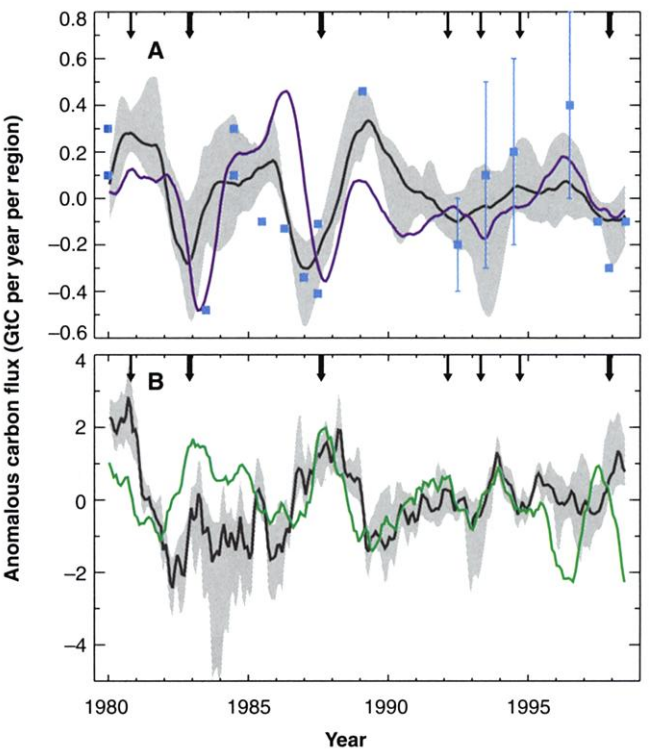

Fig. 2 (left). Inferred anomalous changes in the global land (**A**) and ocean (**B**) carbon fluxes. Black lines are the average of the eight inversions. Shaded areas represent the range of values obtained from the eight sensitivity inversions. For each inversion, we calculated monthly flux anomalies by subtracting the long-term mean flux over the period 1980–1998, and then used a 12-month running mean to deseasonalize the anomalous flux. **Fig. 3 (right).** Carbon balance anomalies of tropical regions. Black lines are the average of the eight inversions. Shaded areas represent the range of values obtained from the eight sensitivity inversions. Thick arrows indicate strong El Niño events documented by minima in the Southern Oscillation Index. Thin arrows indicate weak El Niño conditions. (**A**) Equatorial Pacific region, 20°S to 20°N. The (deseasonalized) flux anomalies derived by the inversion are compared to those predicted by one global three-dimensional ocean carbon model (blue line) that computes changes in ocean circulation and in marine biology (*21*), as well as to those estimated on the basis of ΔpCO_2 measurements compiled in (*17–20*) (blue squares). Uncertainties in the flux estimates (rightmost blue squares) are composed of the seasonal variations of pCO_2 in water, wind speed variability, and wind speed dependence of gas exchange (*18*). Oceanic flux anomalies from the model of (*21*) are averaged over the same regions as the inversion. ΔpCO_2-based flux anomalies are extrapolated to different surfaces of the equatorial Pacific Ocean as described in (*17–20*). (**B**) Tropical land regions, 20°S to 20°N. The deseasonalized flux anomalies derived by the inversion are compared to those predicted by a global biogeochemical model of the terrestrial biosphere [green line, see (*23*)] averaged over the same regions as the inversion. Note that land use–induced and disturbance-induced carbon flux anomalies are not included in the biogeochemical model.

density in the tropics in the early 1980s. The interannual variations estimated from the inversion are in reasonable agreement with those predicted by the global biogeochemical model of (*23*) (r = 0.55, Fig. 3B), except for the period 1996–1998. Note that the inverse estimates combine changes in land use, biomass burning of natural origin and induced by humans, and biogeochemical carbon sources and sinks, whereas the model of (*23*) only accounts for climate-driven biogeochemical effects. Among tropical continents, the Amazon is a major contributor to anomalous carbon balance variations (*24*). However, the partition of the land fluxes within the tropical band can only be tentative, given the absence of sampling stations on the tropical continents and the small magnitude of atmospheric signals (ppm per GtC) caused by strong convective vertical "dilution" of the surface fluxes.

Northern Hemisphere land areas predominantly influenced the carbon flux anomalies during the early 1990s. A strong drop in growth rate occurred during 1992–1993 at mid-northern latitudes (*1*). We invert this signal into an enhanced terrestrial uptake over the Northern Hemisphere continents. Terrestrial carbon storage increased there by 1.4 GtC year^{-1} from the biannual mean in 1989–1990 to that of 1992–1993 (Fig. 4A), in accordance with previous analyses of atmospheric carbon isotopes (*25*) and oxygen data (*26*). Our regional inversions locate the 1992–1993 enhanced terrestrial sink predominantly over North America (~2.0 GtC). This striking result is also directly visible in the CO_2 observations. Figure 4B shows the annual mean difference in CO_2 concentration between Atlantic and Pacific stations, which relates to the North American carbon balance (*27*). The Atlantic stations were 0.5 ppm higher than those in the Pacific during 1989–1990 but were 0.5 ppm lower during 1992–1993 (Fig. 4B). The enhanced North American uptake during 1992–1993 is inferred by all but one of the seven sensitivity runs (*28*). Between 1989 and 1993, North American and Eurasian carbon fluxes are anticorrelated (r = −0.65, see Fig. 4A), but the enhanced uptake over North America remains on average three times the size of the reduced uptake over Eurasia. Moreover, the error correlation between those two regions estimated by the inversion is not significant (r = −0.35), which indicates that the present atmospheric network may be able to correctly separate anomalous changes in Eurasia versus North America in the early 1990s.

The carbon balance of North America has received much attention. We show here that this region experienced a large change in carbon fluxes of 2 GtC in the early 1990s, a change similar in magnitude to the mean annual uptake inferred by Fan *et al.* (*7*) over the period 1988–1992. Although the mean carbon balance of North America appears to be poorly constrained in our eight inversions (*29*), the large flux anomaly that we infer appears fairly robust. This anomalous increase in carbon storage over North America was of short duration; it was followed by a carbon loss of the same magnitude during 1994–1995 (Fig. 4A). A second large negative growth rate anomaly occurred between 1995 and 1997 (see Fig. 4A) that we attribute to an anomalous land uptake of 0.9

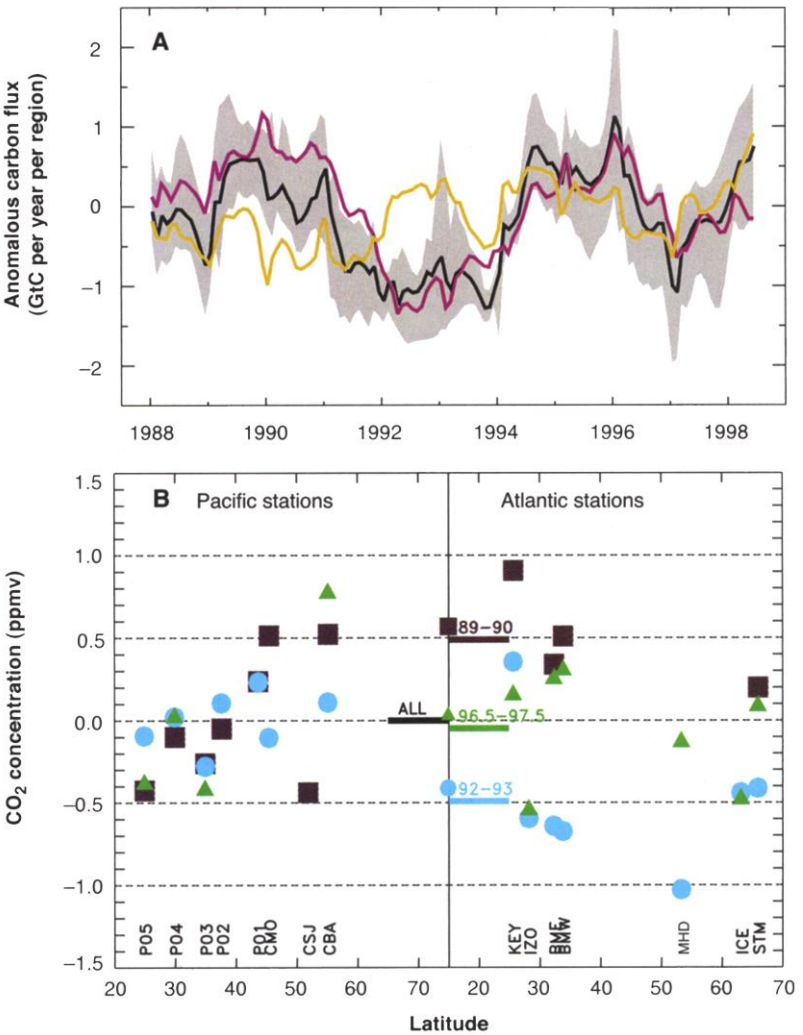

Fig. 4. Carbon balance anomalies of Northern Hemisphere land regions after 1988. (**A**) Terrestrial carbon flux anomalies. Black line is the average of the eight inversions for northern extratropical lands. Shaded area represents the range of values obtained from the eight sensitivity inversions. Flux anomalies are separated between North America (purple line) and Eurasia (orange line). North America corresponds to the aggregated results of the inversion over three regions (temperate, boreal, and arctic in Fig. 1), and Eurasia corresponds to aggregated results over four regions (temperate and boreal Europe, temperate and boreal Siberia in Fig. 1). Note that we restrict this plot to the period 1987–1998 because the partition of land fluxes between Eurasia and North America is constrained by too few sites in the early 1980s (14 sites in 1980 and 20 sites in 1985 for the whole Northern Hemisphere). (**B**) Observed CO_2 concentrations at Eastern Pacific stations (left) and Atlantic stations (right) between 20° and 70°N for two different biannual mean periods (1989–1990 and 1992–1993) and one annual period (1996.5–1997.5). Changes in the difference of concentrations between Pacific and Atlantic sites partly reflect shifts in the carbon balance of North America. For each of the periods 1989–1990, 1992–1993, and 1996–1997, we calculated anomalous concentrations at each site by subtracting the mean concentration calculated using Pacific sites only. This represents anomalies at Atlantic sites compared to Pacific sites [see (*7*), figure 3]. In the Atlantic, each period is summarized by the mean anomaly shown as a horizontal line. In the Pacific, all mean anomalies are zero (the segment "All"). Data are shown for the following locations: BME (32.37°N, 64.65°W), BMW (32.27°N, 64.88°W), CBA (55.20°N, 162.72°W), CMO (45.48°N, 123.97°W), CSJ (51.93°N, 131.02°W), ICE (65.00°N, 24.00°W), IZO (28.30°N, 16.48°W), KEY (25.67°N, 80.20°W), MHT (53.33°N, 9.70°W), STM (66.00°N, 2.00°E), P05 (25.00°N, 154.00°W), P04 (30.00°N, 148.00°W), P03 (35.00°N, 143.00°W), P02 (40.00°N, 138.00°W), and P01 (45.00°N, 131.00°W). For the Pacific Ocean, we exclude sites located too far from the west coast of America (limit of 160°W). For the Atlantic Ocean, we keep all stations between 20° and 70°N. For both oceans, we include the coastal sites (KEY, CSJ, and CMO) and we do not use sites located in the interior of the American continent (UTA, NWR, and ITN).

GtC in the Northern Hemisphere, both over North America (increase of 0.6 GtC) and over Eurasia (increase of 0.3 GtC).

Both 1992 and 1993 were colder years than average over the entire Northern Hemisphere, but North America experienced air temperatures 0.5°C colder than Eurasia in early 1993 (*30*). We find that North American flux anomalies strongly correlate with temperature anomalies over the early 1990s (r = 0.8). A decrease of ecosystem respiration larger than a decrease of photosynthesis could have enhanced carbon uptake over North America during 1992–1993. The global biogeochemical model (*23*), which captured tropical flux anomalies well, fails to reproduce the inferred changes over Northern Hemisphere land ecosystems.

It is important to determine which regions and processes are responsible for interannual changes in the carbon balance of oceans and continents for two reasons. First, the impact of climate variability on the carbon sources and sinks can provide a unique assessment of process models used to predict CO_2 levels in response to emission and climate change scenarios. Second, to detect where CO_2 is being absorbed over land and oceans over the long term, it is necessary to separate interannual variations from long-term mean fluxes. Only when more atmospheric CO_2 measurements become available will it be possible to better understand carbon flux anomalies, especially on land. One of the challenging issues then will be to link this top-down information to local measurements related to the interannual changes in the carbon balance of land ecosystems, such as climate anomalies, land use, and flux and tree-ring data.

References and Notes

1. See figures 6 and 7 in T. J. Conway *et al.*, *J. Geophys. Res.* **99**, 22831 (1994).
2. R. J. Francey *et al.*, *Nature* **373**, 326 (1995).
3. C. D. Keeling *et al.*, *Nature* **375**, 666 (1995).
4. K. Lee, R. Wanninkhof, T. Takahashi, S. C. Doney, R. A. Feely, *Nature* **396**, 155 (1998).
5. C. Le Quéré *et al.*, *Global Biogeochem. Cycles*, in press.
6. A. M. Winguth *et al.*, *Global Biogeochem. Cycles* **8**, 39 (1994).
7. S. Fan *et al.*, *Science* **282**, 442 (1998).
8. P. Bousquet, P. Peylin, P. Ciais, M. Ramonet, P. Monfray, *J. Geophys. Res.* **104**, 26161 (1999).
9. P. Peylin, P. Bousquet, P. Ciais, P. Monfray, in *Inverse Methods in Global Biogeochemical Cycles*, P. Kasibhatla *et al.*, Eds. (American Geophysical Union, Washington, DC, 1999), pp. 295–309.
10. P. J. Rayner, I. G. Enting, R. J. Francey, R. Langenfelds, *Tellus* **51B**, 213 (1999).
11. CO_2 atmospheric data are from the GLOBALVIEW-CO_2 database (available on CD-ROM from Cooperative Atmospheric Data Integration Project–Carbon Dioxide, NOAA Climate Monitoring and Diagnostics Laboratory, Boulder, CO, 1997; also available via anonymous FTP to ftp.cmdl.noaa.gov, path: ccg/CO2/GLOBALVIEW). GLOBALVIEW-CO_2 is a synthesis product that merges data from different air sampling networks. The raw CO_2 concentration data are smoothed in the time domain. Gaps in the data are interpolated, and it is possible to extrapolate the CO_2 time series backward, before the onset of real observations. We have used "interpolated" data but discarded "extrapolated" data, which constitute more than 80% of the GLOBALVIEW-CO_2 database in the early 1980s. Data analysis was performed as described [K. A. Masarie, P. P. Tans, *J. Geophys. Res.* **100**, 11593 (1995)].
12. The 50 sites for which measurements did not begin until after 1994 are excluded from our study. This choice allows us to have at least four consecutive years of raw data for calculating a curve fit to the data at each site (*11*). Two continental sites that are not well represented by the coarse resolution of the transport model are also excluded: Baltic Sea (BAL) and Monte Cimone (CIM). Finally, the station of Azores (AZR) is excluded because of large gaps in the time series (~30%).
13. For further details about the calculation of the deseasonalized trend from the raw data, method and control inversion, multivariate regression coefficient and time lag calculation, net fluxes, and North American carbon balance, see *Science* Online (www.sciencemag.org/cgi/content/full/290/5495/1342/DC1).
14. We adopt temporal and spatial patterns in regional fossil fuel emissions, following the maps of Andres *et al.* [R. J. Andres, G. Marland, I. Fung, E. Matthews, *Global Biogeochem. Cycles* **10**, 419 (1996)] as well as the fossil fuel source magnitude given in *Trends Online, A Compendium of Data on Global Change* (http://cdiac.esd.ornl.gov/trends/trends.htm). Decadal variations in the regional distribution of fossil fuels use are substantial. In the inversion, ignoring such a southward shift in the geographic distribution of the fossil CO_2 source during the 1990s would misallocate an additional terrestrial carbon source of 1.0 GtC over Southeast Asia and an additional terrestrial sink of 0.3 GtC over Eastern Europe and Russia.
15. The seven sensitivity tests are as follows. (i) We used the TM3 model instead of TM2 to test the impact of using a different transport parameterization, which was reported to be a main source of uncertainties when inverting mean fluxes [R. Law *et al.*, *Global Biogeochem. Cycles* **10**, 783 (1996)]. TM3 is based on the same scheme as TM2, but it has a higher vertical and horizontal resolution (5° × 4° × 19 hybrid levels, compared to 7.5° × 7.5° × 9 sigma levels), which produces a CO_2 distribution over continents very different from that of TM2. (ii) We used 1993 meteorological fields instead of 1990 fields to test the impact of interannual variations in the atmospheric transport. (iii) We carried out a test inversion with 16 continental and 14 ocean regions to partly evaluate the impact of spatial discretization of prior sources. (iv) We multiplied all errors on the data by an arbitrary factor of 2, as we may underestimate some observational errors (e.g., representativeness of stations in the model, data selection, network intercalibration). (v) We inverted only the 20 sites covering the full 1980–1998 period to study the effect of the appearance of new data in the assimilation scheme. (vi) We removed the additional constraint on the global ocean uptake. (vii) We inverted deseasonalized data at each site instead of monthly seasonal values to test the impact of the seasonal cycle in the inversion results.
16. For instance, in the inversion, both the TM2 and TM3 models produce fairly similar flux anomalies over tropical lands, but TM2 yields an average net sink of 0.6 GtC year^{-1}, whereas TM3 yields an average net source of 0.2 GtC year^{-1} for the period 1980–1998.
17. For years 1997 and 1998, R. A. Feely, personal communication.
18. R. A. Feely, R. Wanninkhof, T. Takahashi, P. Tans, *Nature* **398**, 597 (1999).
19. R. A. Feely *et al.*, *Deep Sea Res.* **44**, 1851 (1997).
20. C. S. Wong *et al.*, *Tellus* **45B**, 64 (1993).
21. The ocean model is an updated version of that of Le Quéré *et al.* (*5*) and of C. Le Quéré [thesis, Paris VI University (1999)]. The physical model has high resolution at the equator (0.5° × 2.0° of latitude × longitude) and is forced by daily to weekly fields from reanalyzed wind and satellite data. The biogeochemistry model represents the interactions among carbon, nutrients, phytoplankton, zooplankton, and detritus. Initial conditions are based on observations [S. Levitus, M. E. Conkright, J. L. Reid, R. G. Najjar, A. Mantyla, *Prog. Oceanogr.* **31**, 245 (1993); C. Goyet, D. Davies, *Deep Sea Res.* **44**, 859 (1997); C. Goyet, R. Healy, J. Ryan, *Tech. Rep. NDP-076* (Oak Ridge National Laboratory, Oak Ridge, TN, 2000)]. For the computation of air-sea CO_2 fluxes, the atmospheric CO_2 follows the observed monthly average value.
22. The agreement in the Southern Ocean is encouraging and is probably favored by the absence of land and the persistence of westerly winds in this region. The source of atmospheric CO_2 variability is therefore directly attributed to the Southern Ocean. Moreover, both direct and inverse approaches present a negative trend in the anomalous fluxes of −0.4 GtC between 1985 and 1995 for the Southern Ocean (south of 50°S).
23. For land regions, we used the global biogeochemical model CASA-SLAVE [P. Friedlingstein *et al.*, *Global Biogeochem. Cycles* **9**, 541 (1995)]. The terrestrial carbon model (SLAVE) is driven by surface air temperature, precipitation, and solar radiation, and calculates net primary productivity (NPP) according to a light-use efficiency formulation that is a function of temperature and water stress. Litter and soil decomposition follow a methodology similar to CENTURY [W. Parton, D. S. Schimel, C. V. Cole, D. S. Ojima, *Global Biogeochem. Cycles* **7**, 785 (1993)]. Nitrogen limitation and deposition as well as vegetation dynamics are ignored.
24. Amazonian ecosystems act as an anomalous source during 1984–1985, 1987–1988, and 1997, whereas anomalous carbon storage is found in Amazonia during 1985–1986, 1989, 1993, and 1994–1995. No significant correlation between El Niño and carbon storage is observed over the entire period 1980–1998. Although atmospheric inverse modeling does not provide direct insights into biogeochemical processes controlling the year-to-year shifts in the carbon balance of Amazonian ecosystems, we find that enhanced carbon storage positively correlates with precipitation anomalies over the Amazon (r = 0.4) and negatively correlates with temperature anomalies (r = −0.4).
25. P. Ciais *et al.*, *Science* **269**, 1098 (1995).
26. R. F. Keeling, S. C. Piper, M. Heimann, *Nature* **381**, 218 (1996).
27. That changes in the difference between Atlantic and Pacific stations correlate with changes in the North American carbon balance is a necessary, albeit not sufficient, verification of the inversion results (*13*).
28. The inversion where 20 sites are used (*15*) is the only one that changes significantly the inferred 1992–1993 anomalous North American sink (−1.0 GtC year^{-1}) compared to the control run. The addition of new sites to the inversion can alter the consistency of the inferred anomalous changes in carbon fluxes. A significant number of new stations (more than 25) were added in the Northern Hemisphere during the late 1980s. This occurred before the 1992–1993 drop in CO_2 growth rate.
29. Although a mean terrestrial sink north of the Equator is required in our analysis to balance the North minus South CO_2 difference, the partition of that mean sink between Eurasia and North America differs significantly among the eight inversions performed. For instance, the long-term mean carbon flux of North America over 1988–1992 ranges between a sink of 0.3 GtC year^{-1} and a source of 0.6 GtC year^{-1}, which represents in all cases a smaller mean value than the large sink estimated by Fan *et al.* (*7*) over the period 1988–1992.
30. J. Hansen *et al.*, *Geophys. Res. Lett.* **23**, 1665 (1996).

31. We thank M. Heimann for providing LSCE with both TM2 and TM3 models, S. Denning for providing LSCE with SIB2 land surface fluxes, P. Monfray for suggestions and comments about this work, and P. Rayner for many scientific discussions. Supported by the Ministère de l'Education Nationale de la Recherche et de la Technologie (MENRT) under contract 99-1226 and the Commission of the European Community under contract EVK2-CT-1999-00013 (AEROCARB). Computing support was provided by Commisariat à l'Energie Atomique (CEA). This is contribution 0511 of the LSCE.

8 June 2000; accepted 11 October 2000